How wet paper curls

To cite this article: E. Reyssat and L. Mahadevan 2011 *EPL* **93** 54001

A Letters Journal Exploring the Frontiers of Physics

March 2011

EPL, **93** (2011) 54001
doi: 10.1209/0295-5075/93/54001

www.epljournal.org

How wet paper curls

E. Reyssat[1,2(a)] and L. Mahadevan[2]

[1] *Physique et Mécanique des Milieux Hétérogènes, UMR 7636 du CNRS, ESPCI - 10 rue Vauquelin, 75005 Paris, France, EU*
[2] *Engineering and Applied Sciences, Wyss Institute, Harvard University - 29 Oxford St, Cambridge, MA 02138, USA*

received 12 May 2010; accepted in final form 9 February 2011
published online 10 March 2011

PACS 46.70.De – Beams, plates, and shells
PACS 82.30.Rs – Hydrogen bonding, hydrophilic effects

Abstract – When a piece of tracing paper is placed gently on the surface of a bath of water, it rapidly curls up from one edge and rolls up due to the swelling of the side in contact with water. With time, as the swelling front propagates through the thickness of the paper, the paper gradually uncurls itself and eventually straightens out. We analyze the experimental dynamics of rolling and unrolling of the paper and complement these with a minimal theory that explains the basic observations. Our study might be useful in the context of designing biomimetic devices that work as actuators or harness energy from humidity variations.

Introduction. – From pine and spruce cones [1–3] to wheat awns [4], bimetallic thermostats [5] and micro-actuators [6], many natural or man-made slender systems rely on differential expansion of a layered structure for actuation, driven by variations in humidity or temperature. In the world of artificial materials, few surpass the use of paper in its complexity and ubiquity, although it is typically used only as a medium. Since it is particularly sensitive to humidity, paper can be both medium and message; left in an environment of varying humidity such as a bathroom or kitchen, it curls or wrinkles, often irreversibly. Here we describe a more extreme deformation that a piece of thin tracing paper undergoes when placed gently on a bath of water. Contact with the liquid surface causes water to penetrate the paper from one side, a process that induces differential swelling and thus causes the paper to curl; the sheet retracts by rolling up rapidly (fig. 1). Over time, the sheet unfurls and flattens out if it is not long enough to form a closed cylinder; otherwise it either remains closed and curled as surface tension holds it together or unwinds slowly if it happens to drown.

Mechanical probe of the dynamics of water diffusion. – These dynamic shape changes are induced by the movement of water into the porous cellulosic paper which then behaves analogously to a bimetallic thermostat with a small difference. The thin sheet of paper is a single material subject to a differential stimulus (water potential), while the bimetallic strip is a composite subject to the same stimulus (temperature). Differential expansion of the paper layers results in the bending of the sheet, but as water diffuses further into the paper, the differential swelling gradient decreases and the paper starts to uncurl if it is not already a closed cylinder; eventually once the paper is wet all the way through, the sheet flattens out.

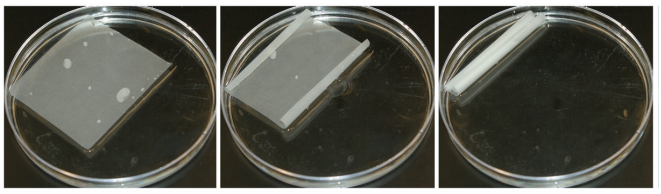

Fig. 1: (Colour on-line) Retraction of an $8 \times 8\,\mathrm{cm}^2$ square of tracing paper ($45\,\mu$m thick) on a water bath. Within a few seconds after contact with water, the paper sheet rolls up into a tight cylinder of radius a few mm. From left to right, the pictures are taken 0.5, 3.5 and 4 s after contact.

Rolling axis. We start with the natural question of the choice of the axis of rolling. Isotropic expansion of the bottom layers of the paper first leads to a biconvex shape, such as the surface of an ellipsoid. However, any deformation into a surface with non-zero Gauss curvature involves stretching of the sheet of paper. Thus while this can arise for very small deformations, it is proscribed as the deformation amplitude increases due to the fact that the energy of stretching relative to bending is large for

(a) E-mail: etienne.reyssat@normalesup.org

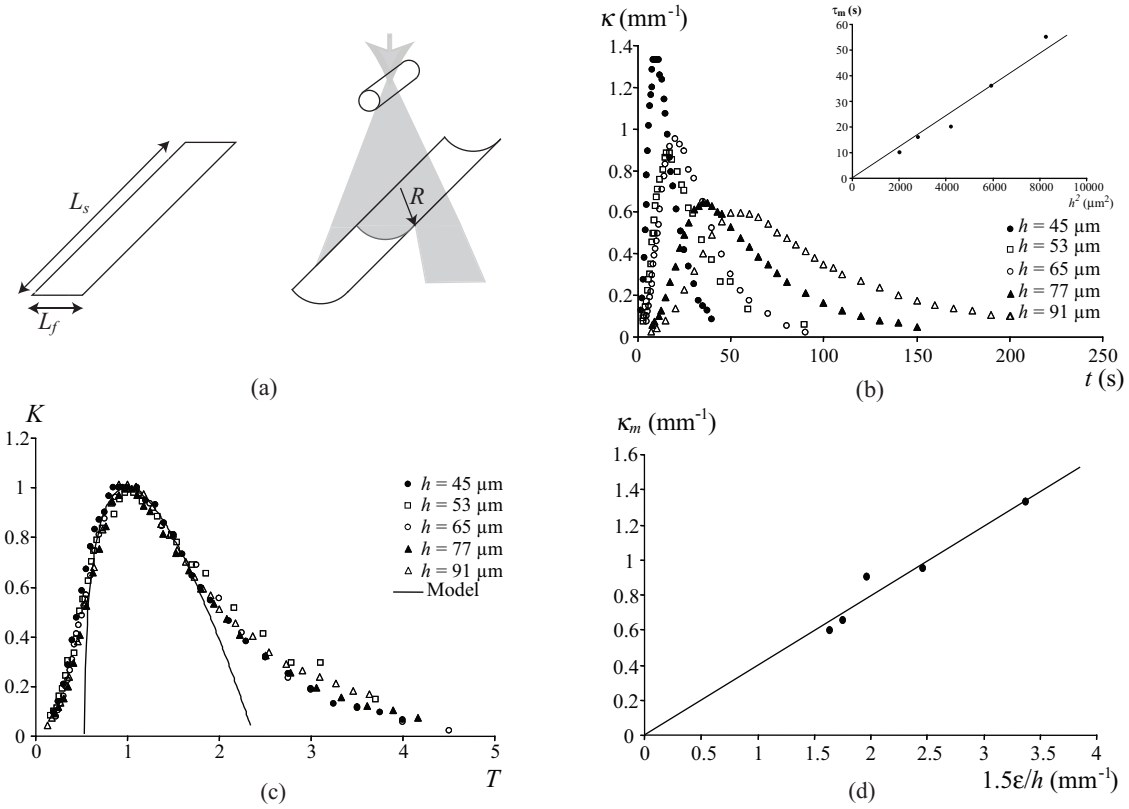

Fig. 2: (a) A narrow piece of paper deposited on water (left) curves upward within seconds, before relaxing to a flat state. We follow changes of curvature $\kappa = 1/R$ using a laser sheet illuminating the strip from above (right). Typically, $L_s \sim 5\,\mathrm{cm}$, and $L_f \ll L_s$ is small enough for the paper not to close into a complete cylinder. (b) Curvature of a paper strip as a function of time following initial contact with water; κ increases strongly, reaches a maximum before relaxing exponentially to zero. The thickness h of tracing paper samples is between 45 and 91 μm. Inset: the time τ_m at which κ is maximum is proportional to h^2, as expected for different diffusive-like water transport mechanisms. (c) Rescaling curvature and time, respectively, by κ_m and τ_m leads to a collapse of the data of panel (b) on a single master curve. The continuous line is an attempt at describing the data by the Timoshenko-Washburn model described in the text, with $n = 1$ and a shift in time. (d) κ_m scales linearly with ε/h, but is about 40% of the expected theoretical value for a simple bilayer structure; the deviation may be partially accounted for theoretically using a continuous variation of the water content through the sheet's thickness.

thin sheets. Thus, strong expansion driven by orthotropic swelling still leads to spontaneous symmetry breaking and the sheet rolls up along an axis that is set by either the presence of small imperfections or the presence of boundaries [7]. In all our experiments, the curling axis is highly repeatable and reveals the pre-existing broken symmetry in the mechanical properties of paper resulting from the manufacturing process that leads to anisotropic alignment of the paper fibers. This then leads to the bending stiffness along the principal directions to typically differ by a factor of 2 or more [8], an effect that increases for thinner paper. The structural anisotropy of paper also implies that the relative expansion upon wetting of different papers is anisotropic, as measured by totally immersing $10 \times 10\,\mathrm{cm}^2$ squares of paper until complete saturation with water. The size of the paper square was measured before and after wetting the samples, enabling to extract the relative expansion ε of the papers. While ε is at most 1% along the fiber axis, it was measured to be between 6 and 10% in the direction perpendicular to the stiffening fibers. The combined anisotropy of the principal bending stiffnesses and swelling sets the axis of the cylinder, and we designate L_s and $L_f \ll L_s$ the lengths along the stiff and more flexible directions.

Coupled water transport and curvature. As water penetrates the floating paper from below, the bottom layers swell first and a layered structure develops. This differential swelling results in the upward bending of the whole sample (fig. 2(a)). Shining a laser sheet on the paper from above enables us to measure the curvature of the sheet by imaging from the side. Figure 2(b) shows the curvature κ of naturally flat strips of different tracing papers as a function of time after first contact with the water bath. After initially bending in response to the transient wetting, the water content becomes homogeneous and the curvature relaxes exponentially to zero as the paper saturates with water. As one expects,

the thinner it is, the faster the paper rolls up, and the tighter the roll. The time τ_m at which curvature reaches its maximum value κ_m increases strongly with the thickness h of paper, in agreement with diffusive-like dynamics: $\tau_m \sim h^2$ (see inset of fig. 2(b)). Rescaling curvature by κ_m and time by τ_m and defining $K = \kappa/\kappa_m$ and $T = t/\tau_m$ allows us to collapse all the data of fig. 2(b) onto a single master curve (fig. 2(c)). This suggests that there is only one time scale in the problem, that of penetration of water into the thickness of the paper structure. The water penetration dynamics is thus decoupled from other possibly time-dependent phenomena such as the kinetics of water absorption by the microscopic cellulose fibers. Similarly, $1/\kappa_m$ is the only relevant spatial scale here.

The simplest attempt at fitting the experimental data of fig. 2(b) is to use Timoshenko's theory for bimetallic thermostats [5] and assume that the paper is made of two distinct layers, a wet one and a dry one. Penetration of water by capillary imbibition, the typical transport mechanism in porous structures such as paper, could yield such a bilayer structure. Moreover, the pseudo-diffusive dynamics of this mechanism, known as the Washburn law [9], is in good agreement with the finding that $\tau_m \sim h^2$. The shape of the sheet is slaved to the water content in it, and can be described via force and torque balance across the section of the paper strip which yields [5]:

$$\kappa = \frac{\varepsilon}{h} f(m,n) \tag{1}$$

where ε is the relative expansion induced by differential swelling of the layers, $m = h_{dry}/h_{wet}$ and $n = E_{dry}/E_{wet}$ are the thickness and Young's moduli ratios of the dry and wet paper layers, and

$$f(m,n) = \frac{6\,(1+m)^2}{3\,(1+m)^2 + (1+mn)\left(m^2 + \frac{1}{mn}\right)}. \tag{2}$$

The maximum curvature of the bilayer is predicted to be linear with the ratio of the relative expansion ε of the material to its thickness h:

$$\kappa_m = 1.5\frac{\varepsilon}{h}. \tag{3}$$

In fig. 2(c), we see that the measured value of κ_m indeed scales linearly with ε/h, but is 40% of that predicted by the simple bilayer model, with $h_{wet} \simeq \sqrt{Dt}$ and $h_{dry} = h - h_{wet}$. The resulting prediction of $\kappa(t)$ may only reasonably well describe the maximum curvature region (fig. 2(c)) with a 0.4 prefactor, a shift in time and for a value of n close to unity, in poor agreement with experiments [10]. Furthermore, the short- and long-time behaviors of $\kappa(t)$ are clearly beyond reach of this simple model.

To understand the reasons for these discrepancies, we note that tracing paper is very dense and the pore connectivity is very low so that classical imbibition mechanisms are likely to be inoperative here. Instead molecular diffusion may be at work, and yields $\tau_m \simeq h^2/D$, D being the molecular diffusion coefficient. Given the values of h (typically 50 μm) and τ_m (of order 30 s) in our experiments, we find that $D \sim 10^{-10}\,\mathrm{m^2\,s^{-1}}$, of the order of magnitude of the molecular diffusion coefficient of water in a gel [11]. To further discriminate between the two possible transport mechanisms, we changed the surface tension γ of the water by adding surfactants. While the molecular diffusion process should be unaffected by changes in γ, the rate of capillary imbibition should change. Figure 3(a) shows that for a drop of surface tension from 72 to 26 mN/m, the bending dynamics of a piece of tracing paper is unchanged, while Washburn's law would imply that the process should be 1.5 times slower. All these point to molecular diffusion being the primary mechanism by which water moves through these narrow pores.

The presence of a molecular diffusion mechanism also implies a smooth gradient of the water content across the thickness of the sample rather than a sharp bilayer

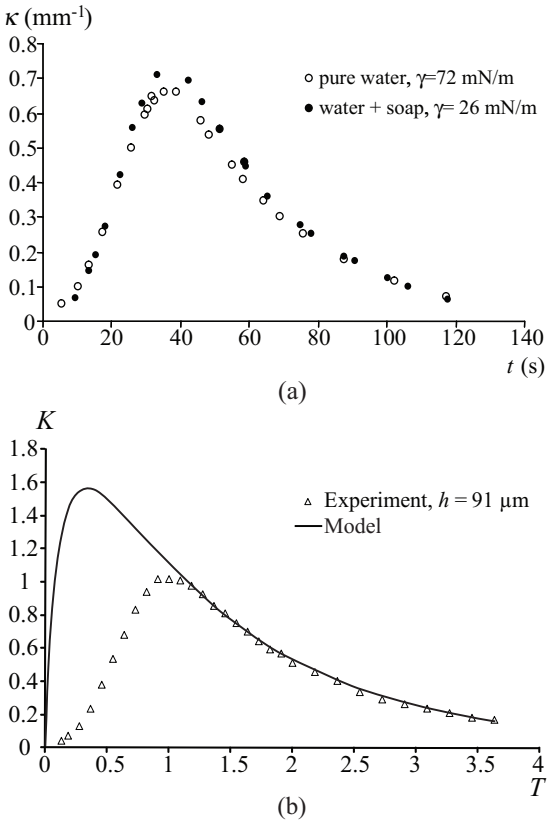

Fig. 3: (a) The bending dynamics of a 77 μm thick paper sample on pure water (surface tension $\gamma = 72\,\mathrm{mN/m}$) and on water with surfactants ($\gamma = 26\,\mathrm{mN/m}$) is identical, showing that water is transported by molecular diffusion rather than capillary imbibition. (b) Rescaled curvature of a paper strip as a function of non-dimensional time as predicted by assuming a smooth diffusive front for the water content profile. At long times, the model fits experimental data very well, while the short-time behavior is due to the complex variation of the modulus as a function of the water volume fraction and the swelling of the paper normal to its plane.

structure. This implies that the vapor concentration obeys a one-dimensional diffusion equation along z, the normal to the surface of the sheet of paper, for the evolution of the water content $\phi(z,t)$, which in general may be written as

$$\frac{\partial \phi}{\partial t} = \frac{\partial}{\partial z}\left(D\frac{\partial \phi}{\partial z}\right), \tag{4}$$

where the water diffusivity $D = D(\phi(z,t))$ in general [12]. In the absence of detailed knowledge of the dependence of the diffusivity on water concentration, we limit ourselves to the case of a non-swelling medium, where $D = \text{const}$, knowing that this is an approximation at best. Then (4) reduces to

$$\frac{\partial \phi}{\partial t} = D\frac{\partial^2 \phi}{\partial z^2} \tag{5}$$

together with the boundary conditions $\phi(z=0,t)=\phi_s$ (the paper side in contact with water is saturated with water) and $\partial\phi/\partial z\ \ (z=h,\ \ t)=0$ (we assume zero flux at the upper surface of the paper), with initial condition $\phi(z,\ \ t=0)=0$ corresponding to a dry sheet. Solving the linear problem using Fourier transforms yields

$$\phi(z,t) = \phi_s\left[1 - \sum_{m=1}^{\infty}\frac{4}{(2m-1)\pi} \times \sin\left(\frac{(2m-1)\pi z}{2h}\right)\exp\left(-\frac{(2m-1)^2\pi^2 Dt}{4h^2}\right)\right]. \tag{6}$$

This result allows us to calculate the curling radius of a strip of material that is inhomogeneous in its thickness in terms of Young's modulus, water content and in-plane relative expansion all of which depend on the z-coordinate through the water content $\phi(z,t)$. We define the neutral layer to be at a location z_n where an undeformed dry homogeneous material at equilibrium, taken as a reference state, remains free of extensional strain. The local extension at any depth due to curvature $\kappa = 1/R$ is then

$$\varepsilon_\kappa(z) = \kappa\,(z - z_n). \tag{7}$$

Moisture in the strip causes it to swell by an amount $\varepsilon_\phi(\phi(z,t))$, depending on the water content of the material $\phi(z)$, so that the local stress at a position z in the cross-section of the strip is

$$\sigma(z) = E(\phi(z,t))\,(\varepsilon_\kappa(z) - \varepsilon_\phi(\phi(z))). \tag{8}$$

For a free strip at equilibrium, the force on any cross-section must vanish, so that

$$F = 0 = \int_0^h E(\phi(z,t))\,(\varepsilon_\kappa(z) - \varepsilon_\phi(\phi(z)))\,\mathrm{d}z, \tag{9}$$

i.e.

$$0 = \kappa\,(I_1 - z_n I_0) - I_{\phi 0}, \tag{10}$$

where $I_i = \int_0^h E(\phi(z,t))z^i\,\mathrm{d}z$ and $I_{\phi i} = \int_0^h E(\phi(z,t))z^i \times \varepsilon_\phi(\phi(z))\,\mathrm{d}z$. Furthermore, the torque on any cross-section must also vanish, so that

$$M = 0 = \int_0^h E(z)z\,(\varepsilon_\kappa(z) - \varepsilon_\phi(\phi(z)))\,\mathrm{d}z \tag{11}$$

or

$$0 = \kappa\,(I_2 - z_n I_1) - I_{\phi 1}. \tag{12}$$

Combining (10) and (12) finally yields an expression for the curvature of the strip:

$$\kappa = \frac{1}{R} = \frac{I_1 I_{\phi 0} - I_0 I_{\phi 1}}{I_1^2 - I_0 I_2}. \tag{13}$$

Here, we have assumed that the time scales for elastic equilibration are very short compared to those for swelling, so that the shape of the strip is slaved to the water content profile, a reasonable assumption. To solve the above equations for the evolving shape of the strip, we need information about the modulus of the fibrous layer $E(\phi(z,t))$ as a function of water content. Studies on the properties of water-laden paper [10] suggests that the mass fraction of water ϕ saturates at about $\phi_s = 0.25$, while the elastic modulus decreases exponentially with water content; here we choose an empirical form that fits the data $E = E_0 e^{-6.7\phi}$, where E_0 is the modulus of dry paper. Then, assuming that $\phi(z,t)$ evolves following the diffusive dynamics (eq. (6)), and that the swelling strain is linear in ϕ, with a maximum value $\varepsilon_\phi(\phi_s)$ (measured to be between 6 and 10%) we can calculate the time-varying curvature κ using eq. (13), as shown in fig. 3(b).

Our results match the experimental data very well at long times (the only adjustable parameter is the diffusion coefficient D of water in paper), consistent with the theoretical model that predicts that at long times, neglecting swelling in the thickness of the paper, $\kappa(t)$ relaxes exponentially to zero as

$$\kappa(t) \simeq C\frac{\varepsilon}{h}e^{-\frac{\pi^2 Dt}{4h^2}}, \tag{14}$$

where $C = 48/\pi^2(4/\pi - 1) \simeq 1.33$. However, the experimentally measured maximum curvature is about 70% of the simple prediction of eq. (3), and as can be clearly seen, the model does not explain the concavity of the $\kappa(t)$ curve at short times. One possible explanation is the swelling of paper normal to its plane upon wetting: the samples we used swell by about 40% along the z-direction. Taking this effect into account, along with the nonlinear kinetics of swelling as embodied in the nonlinear diffusion eq. (4) for $\phi(z,t)$ will clearly change our results without introducing a new time scale, consistent with our experimental evidence which is strongly suggestive of the fact that there is only one time scale in the problem (fig. 2(c)).

Dynamics. – We now turn to the retraction dynamics of larger ($L_f \simeq 20\,\text{cm}$, $L_s \simeq 10\,\text{cm}$) sheets of tracing paper. One end of the strip is free as the other one is held clamped (fig. 4(a)). After deposition on a water bath, nothing visible happens for a few seconds. Then, the free end curves and rolls up on itself at a gradually increasing rate (fig. 4(b)). Retraction goes on at an increasing velocity V reaching up to $20\,\text{cm}\,\text{s}^{-1}$ and is limited by the length L_f of the strips. After complete retraction, the cylinder

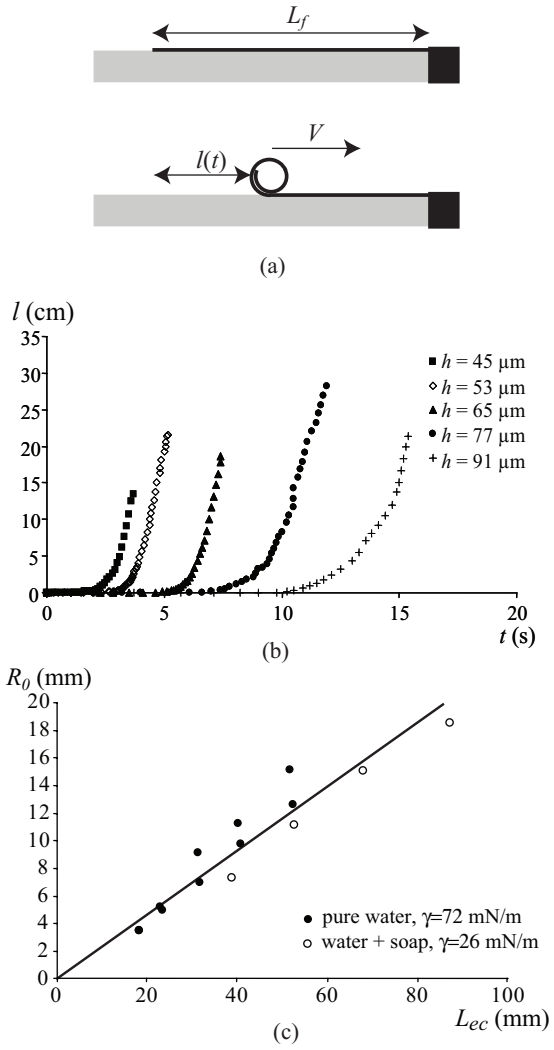

Fig. 4: (a) Schematic of the dynamics of rolling a long sheet of paper. A strip of paper (length L_f) floating on water is held clamped at its right extremity. Upon water intake, the left end curls and retracts, rolling at a velocity V. (b) The retracted paper length as a function of time after deposition on a water bath. The different curves correspond to tracing papers of different thicknesses. (c) The radius R_0 of the rolling cylinder is proportional to the elasto-capillary length L_{ec}. The line of equation $R_0 \simeq 0.23 L_{ec}$ is consistent with the data.

tightens slightly (limited by friction of the wet paper on itself), before slowly unwinding as the water content gradient relaxes. This latter stage usually happens under the water surface, once the wet paper drowns, preventing the sticking of the paper on itself by capillary forces.

Rolling dynamics. As water starts to diffuse into the paper, the initial quasi-static phase corresponds to unobservably small deformations. The curvature becomes significant after a time $\tau_m \sim h^2/D$ (fig. 2(b), inset), the only time scale in the problem suggested by the collapse of our experimental data (fig. 2(c)). Initially, retraction is frustrated by capillary forces that prevent the paper from lifting off from the water surface. Once initiated, retraction speeds up to as much as $20\,\mathrm{cm\,s^{-1}}$, as rolling is driven by moisture-induced curvature change. During the rolling phase of motion, the radius R_0 of the cylinder stays constant: after one full turn is completed, the wet paper sticks to itself through capillary forces and changing R_0 would require to overcome large friction forces. R_0 is correlated to the paper thickness, though not in the same way as κ_m is, being about 5 times larger than the minimal radius of curvature reached by small samples of the same papers. The steady-state value of R_0 is likely set at early times by a competition of bending forces that tend to curl the paper and capillarity preventing the paper from lifting above the water surface. The bending force per unit width of the paper is of order B/R_0^2. The capillary force per unit width is $\gamma \sim 0.07\,\mathrm{N/m}$. Bending overcomes surface tension effects as R_0 reaches the elasto-capillary length $L_{ec} = \sqrt{B/\gamma} \sim 1\,\mathrm{cm}$ [13,14]. We measure B by the gravity loaded cantilever experiment with dry paper samples and deduce L_{ec}. Figure 1(c) shows that R_0 is indeed proportional to L_{ec}, consistent with $R_0 \simeq 0.23 L_{ec}$.

The potential energy available for motion (per unit width of the cylinder and unit length travelled) is of order $B\kappa_0^2$, where B is the bending stiffness of the partially wet sheet (typically of order $10^{-5}\,\mathrm{N\,m}$) and $\kappa_0 = 1/R_0$. Assuming that the rolling motion induces flow in the water bath on a scale $R_0 \sim 1\,\mathrm{cm}$ (as would a fully immersed cylinder translating in a bath at high Reynolds number) the kinetic energy imparted to the water is of order $\rho V^2 R_0$, where $\rho = 1000\,\mathrm{kg\,m^{-3}}$ is the density of water. Balancing kinetic and potential energies yields $V \simeq \sqrt{B/\rho R_0^3} \simeq 0.2\,\mathrm{m\,s^{-1}}$, in qualitative agreement with experiments. Moreover, knowing that $B \sim h^3$ and $R_0 \sim L_{ec} \sim h^{-3/2}$ yields a prediction for the dependence of V on paper thickness h: $V \sim h^{-3/4}$, in qualitative agreement with fig. 4(b) showing that V weakly decreases as h increases.

Edge effects. Although the retraction velocity is relatively independent of the length and thickness of the sheet, it is very strongly dependent on its width L_s. While wide strips of a given paper all retract at similar speeds, the rolling velocity of narrow samples strongly decreases (fig. 5(a)), and the narrowest samples do not even curl at all. Shining a laser sheet parallel to the floating paper reveals the reason for this —the edge of the sheet parallel to the motion direction curls upwards above the water surface (fig. 5(b)) over a distance of approximately 1 cm from the edges. We expect this distance, set by a balance of bending and capillarity, to be the elasto-capillary length L_{ec} again. Curling of the edges acts to stiffen the strip along the direction of motion much as a steel measuring tape is stiffened lengthwise by its transverse curvature. When the retracting front moves, it must straighten the curled edges ahead of it before the sheet can roll up. As we have already discussed, the bending energy gained in rolling a length $\mathrm{d}l$ of paper is of order $B\kappa_0^2 L_s\,\mathrm{d}l$. Straightening the edges has an energy

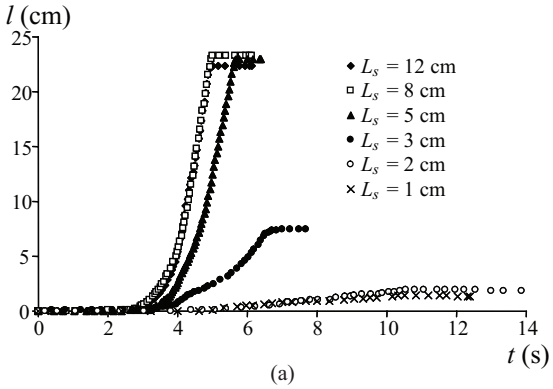

(a)

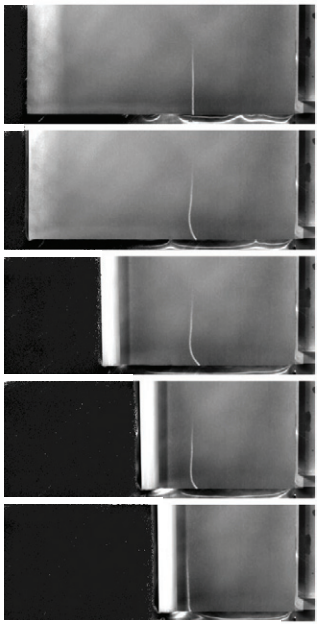

(b)

Fig. 5: (a) Retracted length of 53 μm thick tracing paper samples as a function of time. Narrow strips retract slowly due to the influence of the transverse curvature that predominates in the neighborhood of the edges. (b) 25 cm long and 15 cm wide strip of 65 μm thick tracing paper retracting on water, seen from above. The right end is held clamped while the left extremity is free to curl. The bright line is due to a laser sheet shining from right to left, almost parallel to the water surface. Initially straight when the sheet first contacts water, the line curves as water diffusion induces upward curling along the paper's edges. Before being taken up by the rolling cylinder, the paper flattens as revealed by the straightening of the laser line probe. The pictures were taken 2.6, 5.8, 7.5, 7.8 and 7.9 s after contact with water.

cost proportional to $B_\perp \kappa_\perp^2 L_{ec}\,\mathrm{d}l$, where $B_\perp$ and $\kappa_\perp$ are the bending stiffness and curvature of the strip in the direction normal to motion (in general, they are different from B and κ_0). We see that the difference in driving and resisting energies increases with L_s and vanishes as L_s approaches $L_{ec}(B_\perp\kappa_\perp^2/B\kappa_0^2)$, explaining the observed phenomenology. For wide strips ($L_s \gg L_{ec}$), the driving energy $B\kappa_0^2 L_s$ (per unit length) is lost through hydrodynamic mechanisms that are also linear with L_s, yielding a constant retraction velocity.

Conclusions. – Our study has explained several aspects of the dynamics of a self-rolling wet cigarette both qualitatively and quantitatively. Indeed characterizing how wet paper curls exhibits a rich phenomenology that couples the mechanics of slender bodies to diffusive transport phenomena, hydrodynamics and capillarity. In addition to having intrinsic pedagogical value, the experiment is a macroscopic model for more complex systems such as the bursting of some biological membranes [15,16]. It also suggests simple and robust ways of actuating soft thin films using moisture, and conversely in sensing moisture. An important question that clearly needs addressing now is the nonlinear coupling between swelling, water transport and changes in the elastic properties of the material, which very likely is the reason for the discrepancy between theory and experiment at short times.

* * *

We thank C. Bobtcheff and S. Besson for providing us with materials, Y. Bréchet and J.-F. Bloch for fruitful discussions.

REFERENCES

[1] Dawson C., Vincent J. F. V. and Rocca A.-M., *Nature*, **390** (1997) 668.
[2] Reyssat E. and Mahadevan L., *J. R. Soc. Interface*, **39** (2009) 951.
[3] Fratzl P. and Barth F. G., *Nature*, **462** (2009) 442.
[4] Elbaum R., Zaltzman L., Burgert I. and Fratzl P., *Science*, **316** (2007) 884.
[5] Timoshenko S., *J. Opt. Soc. Am.*, **11** (1925) 233.
[6] Christophersen M., Shapiro B. and Smela E., *Sens. Actuators B*, **115** (2006) 596.
[7] Mansfield E. H., *Proc. R. Soc. London, Ser. A*, **288** (1965) 396.
[8] Baum G. A., Habeger C. C. and Fleischman E. H., IPC Technical Paper Series, No. 117 (1981), `http://hdl.handle.net/1853/2848`.
[9] de Gennes P.-G., Brochard-Wyart F. and Quéré D., *Gouttes, bulles, perles et ondes* (Belin, Paris) 2005, p. 118.
[10] Nissan A. H., *Macromolecules*, **9** (1976) 840.
[11] Zhang H. and Davison W., *Anal. Chim. Acta*, **398** (1999) 329.
[12] Philip J. R., *Annu. Rev. Fluid Mech.*, **2** (1970) 177.
[13] Cohen A.E. and Mahadevan L., *Proc. Natl. Acad. Sci. U.S.A.*, **100** (2003) 12141.
[14] Bico J., Roman B., Moulin L. and Boudaoud A., *Nature*, **432** (2004) 690.
[15] Abkarian M., Massiera G., Berry L., Roques M. and Braun-Breton C., to be published in *Blood* (2010) DOI 10.1182/blood-2010-08-299883.
[16] Mabrouk E., Cuvelier D., Brochard-Wyart F., Nassoy P. and Li M.-H., *Proc. Natl. Acad. Sci. U.S.A.*, **106** (2009) 7294.